Supporting Information

Fast Magic-Angle-Spinning ^{19}F Spin Exchange NMR for Determining Nanometer ^{19}F–^{19}F Distances in Proteins and Pharmaceutical Compounds

Matthias Roos, Tuo Wang, Alexander A. Shcherbakov, and Mei Hong*

Department of Chemistry, Massachusetts Institute of Technology, 170 Albany Street, Cambridge, MA 02139

CSA-driven ^{19}F rotational resonance

When the MAS frequency matches the isotropic chemical shift difference between two resonances,

$$k\omega_r = \Delta\delta_{iso} := \left|\delta_{iso,2} - \delta_{iso,1}\right| \quad (k = 1, 2) \ , \tag{S1}$$

rotor-driven polarization transfer will occur, which speeds up spin diffusion. For spins with the same isotropic chemical shift but different tensor orientations, the chemical-shift offset that needs to be compensated for can be characterized by the average fluctuation amplitude of the *instantaneous* chemical shift difference,

$$2\Delta H(t) = H_{CS,2}\left(\theta_2(t), \phi_2(t)\right) - H_{CS,1}\left(\theta_1(t), \phi_1(t)\right) \ , \tag{S2}$$

where

$$H_{CS,i}\left(\theta_i(t), \phi_i(t)\right) = \delta_{iso} + \Delta\delta\left\{\frac{1}{2}\left(3\cos^2\theta_i(t) - 1\right) - \frac{1}{2}\eta\sin^2\theta_i(t)\cos 2\phi_i(t)\right\} \tag{S3}$$

is the chemical shift Hamiltonian of spin i, $\theta_i(t) = \theta_i\left(\Omega_i, \gamma(t)\right)$ and $\phi_i(t) = \phi_i\left(\Omega_i, \gamma(t)\right)$ are the polar and azimuthal angle of the chemical shift tensors in the laboratory frame, and Ω_i is the set of Euler angles relating the laboratory frame to the crystal-fixed frame that rotates by an angle $\gamma(t) = \omega_r t$ about the rotor axis. Inserting

$$\theta_2(t) = \theta_1(t) + \Delta\theta \ , \quad \phi_2(t) = \phi_1(t) + \Delta\phi \tag{S4}$$

into Eq. (S2) and making use of the fact that MAS gives isotropic averages of anisotropic interactions such as the CSA, the characteristic chemical-shift difference fluctuation amplitude, $\sqrt{\langle \Delta H^2 \rangle}$, is calculated as the isotropic average over $\theta_1(t)$ and $\phi_1(t)$. The resulting equation reveals a negligible dependence on $\Delta\phi$, which will henceforth be neglected by setting $\Delta\phi = 0$. In practice, $\Delta\theta$ can be identified as the angle between the largest chemical shift principal axis of the two spins. Then, the MAS frequency under which CSA-driven rotational resonance occurs is, for the condition $k = 1$,

$$\omega_{r,opt} \cong \sqrt{\langle \Delta\mathcal{H}^2 \rangle} \cong \frac{|\Delta\delta|}{8\sqrt{15}} \sqrt{\left(18+\eta^2\right)\left(15+\cos 2\Delta\theta\right)\sin^2\Delta\theta}\,. \qquad \text{(S5)}$$

Since $\Delta\delta$ is usually given in units of Hz and not in rad s^{-1}, $\omega_{r,opt}$ in Eq. (S5) has been replaced by $\nu_{r,opt}$ in the main text to avoid confusion with the factor of 2π.

Motivation for, and limitations of, the chemical-shift bias correction

For spin pairs with chemical-shift differences larger than their dipolar coupling, spin polarization exchange occurs with reduced probability ("weak-coupling limit"). Here, dipolar-mediated spectral overlap can be significantly reduced, and energy-conserving flip-flops are hindered.

The spectral overlap between two resonances is governed by their isotropic chemical-shift difference and their spectral lineshape. While Lorentzian curves are observed in solution NMR in the limit of vanishing dipolar couplings, static solid-state NMR resonances are commonly associated with Gaussian peaks. Between these two limiting scenarios, MAS and imperfect cancelation of dipolar couplings often leads to spectral lineshapes that are best described by a superposition of a Gaussian and Lorentzian curve (**Figure S1a)**.

The peak overlap between two Lorentzian curves,

$$f_{L,i}(\omega-\omega_i) = \frac{1}{\pi}\frac{\sigma_i}{\sigma_i^2+\left(\omega-\omega_i\right)^2}, \qquad \text{(S6)}$$

is determined by

$$F_L(0) = \frac{\tilde{g}_0\sigma_\Sigma}{\pi\left(\sigma_\Sigma^2+\Delta\delta_{iso}^2\right)} \approx \frac{f_0}{\Delta\delta_{iso}^2} \quad \text{for} \quad \Delta\delta_{iso}^2 \gtrsim 5...10\,\sigma_\Sigma^2\ , \qquad \text{(S7)}$$

where $f_0 := \tilde{g}_0\sigma_\Sigma/\pi$. $\Delta\delta_{iso} = |\omega_i-\omega_j|$ and $\sigma_\Sigma := \sigma_i+\sigma_j$ are the isotropic chemical-shift difference between the two resonances and the sum of their individual half-widths at half-maximum, respectively. The parameter $\tilde{g}_0 = \tilde{g}_{CORD}\tilde{g}_{MAS}$ is a dimensionless phenomenological correction factor that accounts for CORD, MAS or CSA-related effects, and will be addressed below.

Gaussian peaks, on the other hand, yield a Gaussian spectral overlap:

$$F_{\mathrm{G}}(0) = \frac{\tilde{g}_0}{\sqrt{2\pi}\,\hat{\sigma}_\Sigma} \exp\left(-\frac{\Delta\delta_{\mathrm{iso}}^2}{2\hat{\sigma}_\Sigma^2}\right) \quad , \quad \hat{\sigma}_\Sigma^2 := \sigma_{\mathrm{i}}^2 + \sigma_{\mathrm{j}}^2 \;=\; \sigma_\Sigma^2 - 2\sigma_{\mathrm{i}}\sigma_{\mathrm{j}} \quad . \tag{S8}$$

For well resolved peaks that resemble a superposition of a Gaussian and a Lorentzian lineshapes, the spectral overlap will be dominated by the contribution of the Lorentzian lineshape as soon as $\Delta\delta_{\mathrm{iso}} > 2\sigma_\Sigma$, thus $k_{\mathrm{SD}} \approx 0.5\pi\omega^2 F_{\mathrm{L}}(0)$. This simple relationship yields an excellent agreement with the data recently published by Wittmann et al. (**Figure S1b**) [1], who report a decrease of the ^{1}H spin diffusion efficiency with increasing ^{1}H chemical-shift differences under 100 kHz MAS. For such high spinning frequencies, reduced dipolar couplings yield ^{1}H resonances of about 200 Hz linewidth or less, resulting in reduced or no spectral overlap for several ^{1}H peaks. In the limit of weak dipolar couplings yielding Lorentzian-like peaks, $k_{\mathrm{SD}} \approx 0.5\pi\omega^2 F_{\mathrm{L}}(0)$ will also apply if $\Delta\delta_{\mathrm{iso}} \lesssim 2\sigma_\Sigma$. Then, k_{SD} is nearly independent of $\Delta\delta_{\mathrm{iso}}$, which is depicted in **Figure S1b)**.

Recoupling of ^{19}F–^{1}H dipolar couplings broadens ^{19}F resonances, yielding increased spectral overlap for spins with distinct isotropic chemical shifts. Comparing CORD polarization transfer with PDSD (**Table S1**) reveals a 10 to 100-fold increase in the polarization transfer efficiency, reflecting increased spectral overlap ($\tilde{g}_{\mathrm{CORD}} \sim 10^1 - 10^2$), with an average of $\langle \tilde{g}_{\mathrm{CORD}} \rangle \geq 40$.

MAS and the large ^{19}F CSA affect the effective overlap integral through the instantaneous, orientation-dependent chemical shift of each spin that is periodically modulated in each rotor period. For resonances experiencing temporarily reduced chemical-shift differences, or even transient level crossings if the combined CSA span is larger than the isotropic shift difference, spin polarization exchange will be more efficient [2]. The results on 5F-Trp and the data in ref. [2] suggest an MAS-driven increase of the effective spectral overlap of up to $\langle \tilde{g}_{\mathrm{MAS}} \rangle \lesssim 2-3$, such that $\langle \tilde{g}_0 \rangle \sim \langle \tilde{g}_{\mathrm{CORD}} \rangle \cdot \langle \tilde{g}_{\mathrm{MAS}} \rangle \sim 10^2$.

For well-resolved peaks, the enhancement of spin diffusion rates due to CORD and/or MAS and CSA effects can be expected to be only weakly correlated with σ_Σ. Then, the covariance of σ_Σ and $\tilde{g}_0$ is small, and $\langle \tilde{g}_0 \sigma_\Sigma \rangle \approx \langle \tilde{g}_0 \rangle \langle \sigma_\Sigma \rangle$. Note that $\langle \sigma_\Sigma \rangle = 2\langle \sigma_{\mathrm{i}} \rangle_{\mathrm{i}}$ equals the average full-width half-maximum linewidth of the ^{19}F resonances.

The calibration constant *c* reported in the main text is an average over several ^{19}F spin pairs:

$$c = \left\langle \frac{1}{2}\pi f_0 \cdot \omega^2 r^6 \right\rangle \;\approx\; \frac{\langle \tilde{g}_0 \rangle \langle \sigma_\Sigma \rangle}{10} \cdot \left(\frac{\mu_0}{4\pi}\gamma^2\hbar\right)^2 \quad , \tag{S9}$$

and needs to be determined empirically because of the uncertainty in $\langle \tilde{g}_0 \sigma_\Sigma \rangle$. On the right-hand side in Eq. (S5), the angular part of dipolar couplings, $\frac{1}{4}\left(3\cos^2\theta - 1\right)^2$, has been replaced by its powder-

averaged value of 1/5. Considering $\langle\sigma_\Sigma\rangle$: 10^3 Hz for sake of simplicity (1.8 ppm at $\omega_0 = 564$ MHz) and $\tilde{g}_{\mathrm{CORD}} \approx 10^2$, the calibration constant c for ^{19}F CORD polarization transfer is predicted to be in the order of 10^{14} s^3/Å^6, which matches the experimental finding for F–F spin pairs.

The chemical shift bias correction used in the main text, $F_{\mathrm{L}}(0) \approx f_0 / \Delta\delta_{\mathrm{iso}}^2$, requires well-resolved peaks. For resonances with peak overlap, deviations from $c \sim 10^{14}$ s^3/Å^6 are expected. These deviations not only result from the neglect of σ_Σ^2 in the denominator of Eq. (S7), but are also due to a considerable change in $\langle\tilde{g}_0\rangle$. For spin pairs with spectral overlap, ^{19}F–^{1}H dipolar recoupling reduces the spin diffusivity. For 5F-Trp at 25 kHz MAS, $\tilde{g}_{\mathrm{CORD}} \approx 0.1$ (see **Table 2**), which is associated with a 10^3-fold lower spin polarization exchange efficiency for PDSD compared to CORD polarization exchange between spectrally resolved spin pairs. This situation applies to the Y3–Y45 spin pair in GB1, where the predicted thousand-fold decrease in spin diffusivity is in close agreement with the experimental data.

Peaks with considerable spectral overlap are reminiscent of the strong-coupling limit. For dipolar couplings stronger than or comparable to the chemical shift differences, chemical shifts bias will be less important, as is well established for ^{1}H spin diffusion (except under very fast MAS [1]). Here, dipolar couplings are sufficient to provide adequate spectral overlap, rendering spin diffusion insensitive to the local chemical environment. This situation is exemplified by the F_M–F_P spin pair in sitagliptin (see main text).

We finally note that for spins with distinct isotropic chemical shifts, long-distance dipolar couplings will most often be in the weak-coupling limit, and chemical-shift bias should be corrected.

Table S1. Best-fit result of the spin polarization exchange times τ_{PDSD} and $\tau_{CORD,}$ and the ratio of the two time constants. Fitting uncertainties of the exchange times are about 10% of the reported value for PDSD, and ±0.1 ms for CORD.

Spin pair	**τ_{PDSD} (ms)**	**τ_{CORD} (ms)**	**τ_{PDSD}/ τ_{CORD}**
F_3F_3	198	12.7	16
F_3O	169	18.9	9
F_3P	170	10.3	17
F_3M	>1500	12.5	>120
OO	210	20.0	11
OF_3	154	17.0	9
OP	539	40.6	13
OM	>1500	18.5	>81
MM	778	13.8	56
MF_3	1210	8.8	138
MO	>1500	44.3	>34
MP	214	6.7	32
PP	155	9.1	17
PF_3	105	8.8	12
PO	406	17	24
PM	281	6.9	41
Average			**>40**

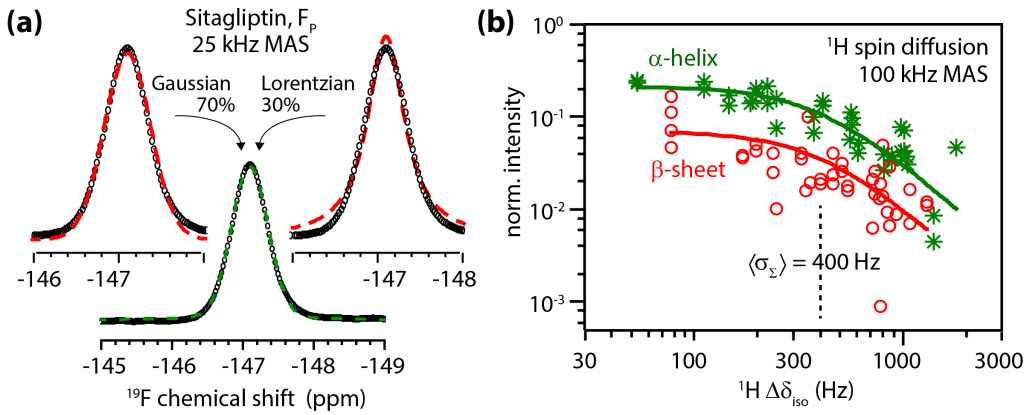

Figure S1. **(a)** Lineshape of solid-state NMR resonances illustrated using the F_P peak (points) of sitagliptin under 25 kHz MAS. Neither a pure Gaussian (G, left) nor a pure Lorentzian (L, right) lineshape (lines) matches the experimental spectrum well, but a 70 : 30 G : L superposition of the two (bottom) yields sufficient agreement with the experimental data. **(b)** Cross-peak intensities of amide protons of neighboring residues in ubiquitin α-helices (star symbols) and β-sheets (circles), observed after a 20-ms ^{1}H spin diffusion mixing period. Cross-peaks in each domain have similar distances, and are assumed to be in the initial build-up regime, where $I(t_{mix})/I_0 \approx k_{SD} t_{mix} = k_0 F_L(0)$ (lines). Note that k_0 was the only fitting parameter and serves to adjust the vertical position of the fitting curves. Data reproduced from ref. [1] and re-plotted on a double-logarithmic scale.

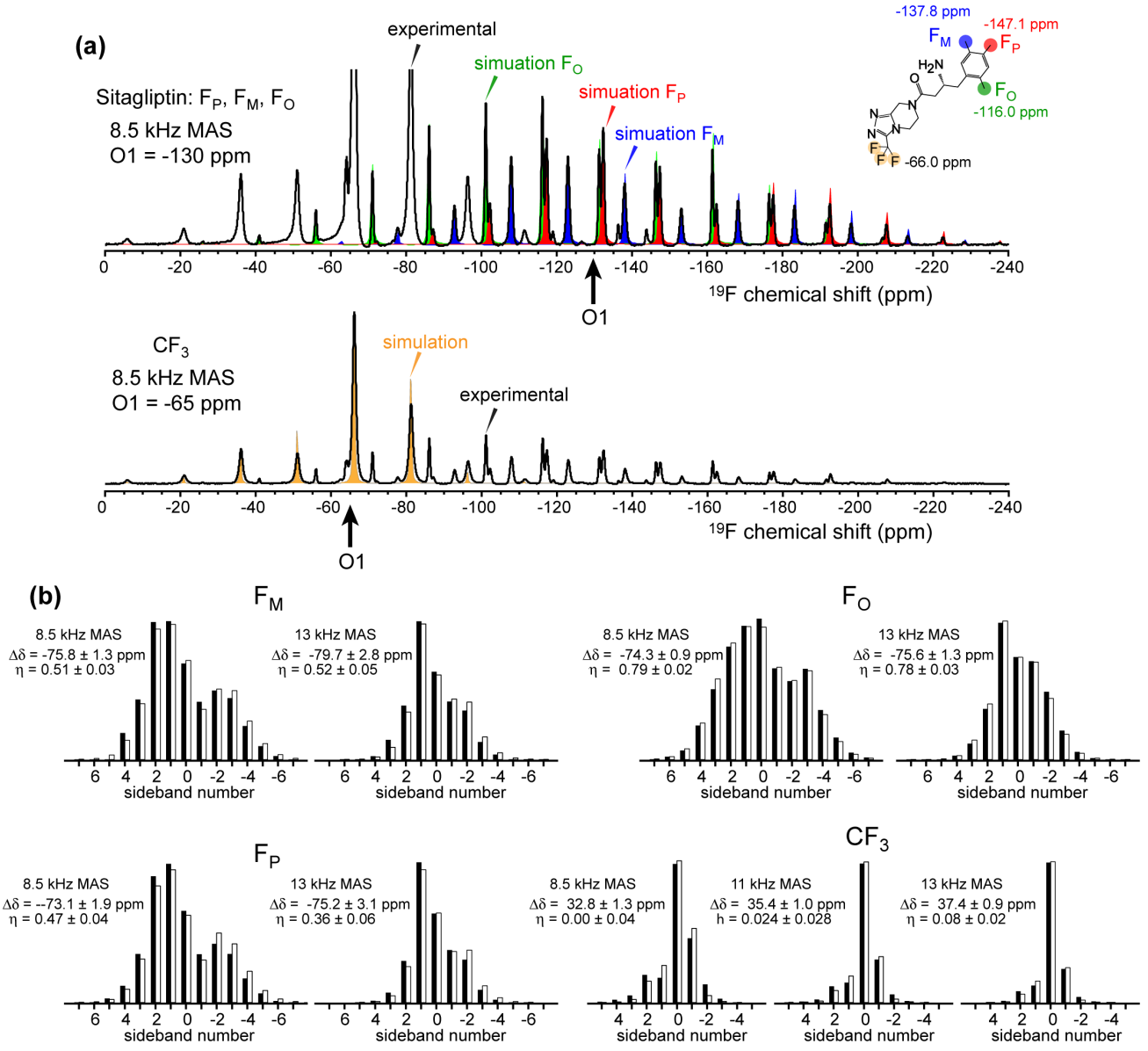

Figure S2. Representative CSA sideband spectra for extracting the ^{19}F chemical shift tensor parameters. The four-spin sitagliptin spectra are shown. **(a)** ^{19}F spectra measured under 8.5 kHz MAS, with the ^{19}F carrier frequency at -130 ppm (top) and -65 ppm (bottom), to obtain accurate intensity patterns of aromatic and CF_3 groups, respectively. Best-fit simulations for the four ^{19}F sites using the CSA principal values obtained from the Herzfeld-Berger analysis are overlaid with the experimental data. **(b)** Herzfeld-Berger analysis of the sideband manifold of the four ^{19}F spins. Experimental spectra were obtained at multiple MAS frequencies to obtain accurate anisotropy parameter Δδ and asymmetry parameter η.

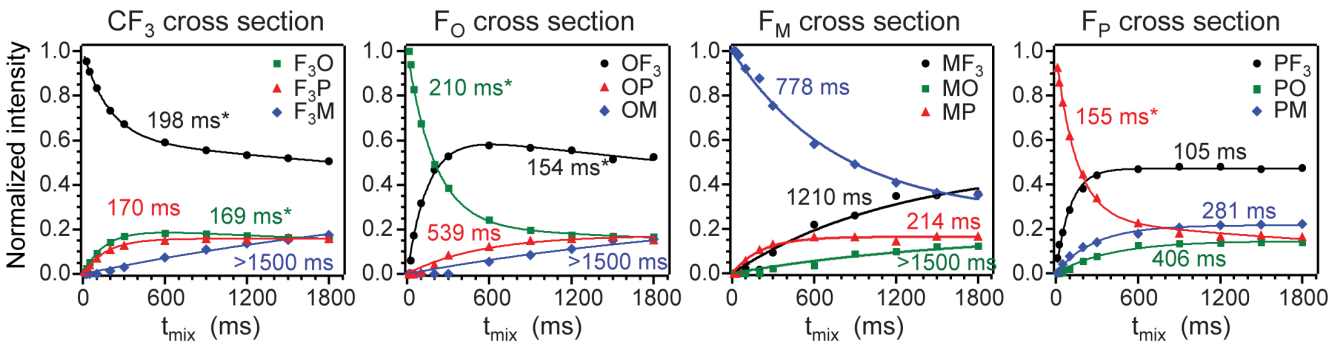

Figure S3. ^{19}F PDSD buildup curves of sitagliptin. For very slow cross-peak buildup curves, only the lower-bound polarization exchange time constant can be estimated. Fitted exchange time constants marked by an asterisk indicate that T_1 relaxation has been taken into account, by multiplying the exponential buildup or decay curves by e^{-t_{mix}/T_1}.

References

1. Wittmann, J. J.; Agarwal, V.; Hellwagner, J.; Lends, A.; Cadalbert, R.; Meier, B. H.; Ernst, M., Accelerating proton spin diffusion in perdeuterated proteins at 100 kHz MAS. *J. Biomol. NMR* **2016,** *66*, 233-242.
2. Roos, M.; Micke, P.; Saalwächter, K.; Hempel, G., Moderate MAS enhances local ^{1}H spin exchange and spin diffusion. *J. Magn. Reson.* **2015,** *260*, 28-37.